

Possible role of microRNA miRNA-IL-25 interaction in mice with ulcerative colitis

Jun Yao^a, Ruo-yu Gao^a, Ming-han Luo^a, Cheng Wei^a, Ben-hua Wu^a, Li-liangzi Guo^a, Li-sheng Wang^a, Jian-yao Wang^b, and De-feng Li^a

^aDepartment of Gastroenterology, Jinan University of Second Clinical Medical Sciences, Shenzhen People's Hospital, Shenzhen, Guangdong Province, China; ^bDepartment of General Surgery, Shenzhen Children's Hospital, Shenzhen, Guangdong Province, China

ABSTRACT

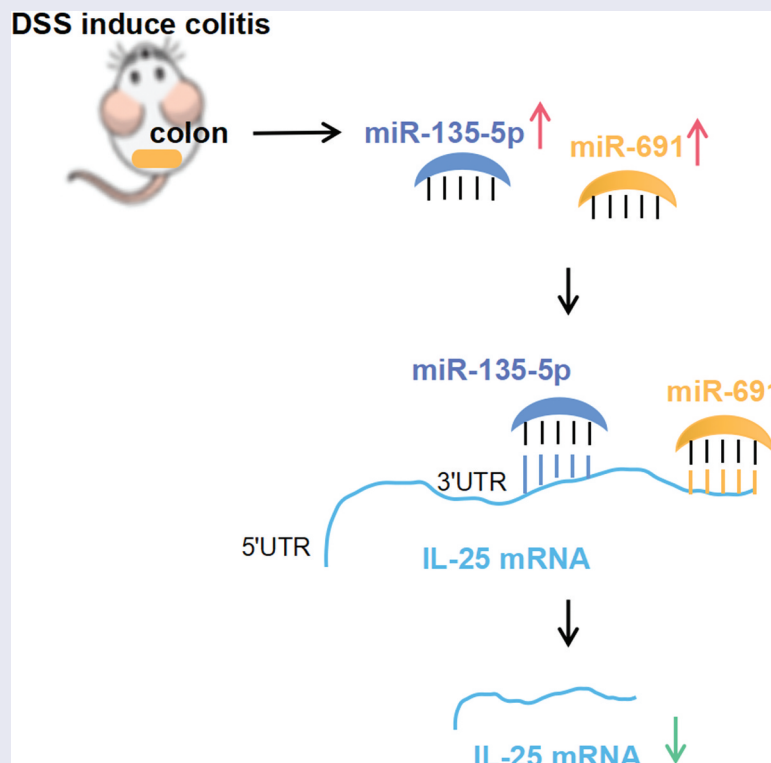
Background: The regulatory network of ulcerative colitis (UC)-associated miRNAs is not fully understood. In this study, we aim to investigate the global profile and regulatory network of UC associated miRNAs in the context of dextran sulfate sodium (DSS). **Methods:** UC was induced in C57BL mice using DSS. Differentially expressed miRNAs were screened by RNA sequencing and subjected to the Kyoto Encyclopedia of Genes and Genomes Pathway enrichment analysis. RT-qPCR was used to verify the differential expression of miRNAs and candidate target mRNA. Luciferase reporter vector bearing a miRNA binding site was constructed to verify the binding site of the miRNA on mRNA. **Results:** A total of 95 miRNAs (31 were up-regulated and 64 were down regulated) differentially expressed in the colonic tissues of the UC mice. Among the differentially expressed miRNAs, IL-25 pathway genes were enriched. Subsequent RT-qPCR confirmed a decreased expression of IL-25 and a significant up regulation of IL-25 target miRNAs including mmu-miR-135b-5p, mmu-miR-7239-5p and mmu-miR-691 in UC mice. **Conclusion:** Using the luciferase assay, we verified the binding sites of mmu-miR-135b-5p and mmu-miR-691 to the IL-25 3'UTR. In conclusion, mmu-miR-135b-5p:IL-25 and mmu-miR-691:IL-25 interactions are important pathways that may exert a protective role in UC.

ARTICLE HISTORY

Received 17 June 2020
Revised 29 July 2020
Accepted 29 July 2020

KEYWORDS

MicroRNA; ulcerative colitis; miR-135b-5p; miR-691; IL-25



Introduction

Ulcerative colitis (UC) is an idiopathic chronic inflammatory disease and is one of the two major types of inflammatory bowel disease (IBD). It is estimated that the direct medical cost of UC ranges from \$6217 to \$11477 (per patient per year) in the United States and €8949 to €10395 in Europe [1]. Although UC is a costly and life-threatening disease for patients with acute severe ulcerative colitis in western countries [1], the pathogenesis of UC remains unknown. Genetic and epigenetic factors are believed to be involved in UC pathogenesis [2].

MicroRNA (miRNA) is an endogenous short (about 21 nt long) non-coding RNA that performs its function primary by binding to the 3'UTR of its target mRNA with the seed sequence (5' end 2–8 nt), resulting in targeted mRNA level and protein translational inhibition [3]. Increased evidence suggests that miRNA is one of the important pathogenic factors of inflammatory diseases [4,5]. In UC, miRNAs are dysregulated in human mucosal and epithelial tissues [6–8], playing an important role in the regulation of the intestinal epithelial cell barrier environment and homeostasis, thus regulating inflammation [9,10]. Although studies have revealed miRNA expression profiles in UC patients, including active and/or inactive intestinal mucosa, blood samples [6,11,12], and in special populations, such as a pediatric population [7]. However, most of these studies are based on microarray technology that cannot reflect the global change in UC expression profiling. At the same time, it is difficult to completely control the basic disease context of the recruited patients. Therefore, miRNA profiles based on the experimental model and performed on high-throughput sequencing platform may enhance our understanding of miRNA-mRNA regulatory pathways in UC.

UC is characterized by chronic relapsing intestinal inflammation. Dysregulation in the inflammation-related pathways is a characteristic of this disease. Previously, several studies have suggested inflammation-associated miRNA-mRNA interaction regulatory relationship in UC. For example, microRNA-31 and miR-155 target interleukin 13 receptor α -1 [13]. miR-4284 and miRNA-141 bind directly to the CXCL5 3'UTR [7,14]. However, more miRNA/mRNA pathways, especially the regulatory network

between UC-related miRNAs and inflammation-related pathways, require investigation.

In this study, we investigated the expressed miRNA profiles using high-throughput sequencing based on a dextran sulfate sodium (DSS)-induced UC mouse model. Next, we analyzed the major enrichment pathways of miRNAs to assess the inflammation-associated miRNAs-mRNA regulatory relationship.

Materials and methods

Cell culture

HEK-293 cells (ATCC, Rockville, MD) were cultured in DMEM (Invitrogen, CA, USA) medium containing 10% fetal bovine serum in a 5% CO₂ incubator at 37°C.

Establishment of a DSS-induced UC mouse model

UC mouse model was induced via administration of DSS. A total 12 C57BL/6 mice (6–8 weeks old) were randomly resigned to the normal feeding group (NC) or the DSS feeding group (DSS). DSS mice were administrated 2.5% DSS (Biochemicals, CA, USA) in their drinking water for 7 days to induce acute UC. NC mice with regular drinking were used as vehicle controls. The disease activity index (DAI) was scored as per the following scoring system: Weight: 0, no loss; 1, 5%–10% lost; 2, 10%–15% loss; 3, 15%–20% loss; and 4, >20% loss; stool: 0, normal; 2, loose stool; and 4, rib, diarrhea; and bleeding: 0, no blood; 1, presence of blood; 3, obvious blood; and 4, gross blood. DAI and body weight were recorded from day 0 to day 14 after DSS treatment. Spleen weight loss and colon length were determined at day 7 after DSS treatment. To determine the histological change after DSS treatment, the distal colon was fixed in 4% paraformaldehyde to prepare paraffin-embedded blocks on day 7 after DSS treatment. Hematoxylin and eosin (H&E) were used to assess the histological change after DSS treatment. All animal experiments were reviewed and approved by the Jinan University Animal Medical Ethics Committee, China.

MiRNA sequencing and bioinformatics

Total RNA was isolated from the intestinal tissue of two DSS-induced UC mice and two control mice at day 14 post DSS treatment using TRIzol Reagent (Thermo Fisher Scientific, MA, USA) as per the manufactures' instructions. Total RNA was qualified using Agilent Bioanalyzer 2100 (Agilent, Agilent Technologies, CA, USA). Next, small RNA libraries were generated with a TruSeq Small RNA Sample Preparation Kit (Illumina, CA, USA) as per the manufacture's recommendation, and the libraries were qualified with Agilent Bioanalyzer 2100. RNA sequencing was performed on an Illumina HiSeq2000 platform (Illumina).

The raw data released from the HiSeq2000 platform were filtered to remove low-quality reads. Reads with 'adapter-only' or unclipped were also discarded. The remaining reads were aligned to the mouse NCBI37/mm9 genome sequencing using SOAP V2.0. miRNA was predicted and annotated using NCBI Refseq data and NCBI Genbank data (<http://www.ncbi.nih.gov>). miRNAs that meet the criteria of fold change ≥ 2 and with a $P < 0.01$, were identified as differentially expressed miRNAs in UC mice.

To predict potential function of the differentially expressed target gene of miRNAs that may be involved, the Kyoto Encyclopedia of Genes and Genomes (KEGG) pathway analysis was conducted using open-source R package. Q (adjusted P value) < 0.001 was considered to indicate significant enrichment. Candidate miRNA targets were predicted using Targetscan and the interaction network of miRNA-mRNA was visualized by R software.

Real-time quantitative RT-PCR (RT-qPCR)

The expression of miRNA and mRNA were validated using RT-qPCR. First, total RNA was reverse transcribed using QuantiTect Reverse Transcription Kit (Qiagen, Valencia, CA) and amplified using QuantiTect SYBR Green RT-PCR Kit (Qiagen) as per the manufactures' instructions. The amplification was performed on an ABI 7500 real-time PCR system (Applied Biosystems, CA, USA). The relative expression of miRNA and mRNA was calculated using the $2^{-\Delta\Delta C_t}$ method. U6 and GAPDH was used as an internal control. Primers used for RT-qPCR are listed in Table 1.

Table 1. Primer sequence used in this study.

Primer	Sequence (5' to 3')
mmu-miR-761	GCAGCAGGGTAAAAGTATCAA
mmu-miR-7002-5p	TTGGCTTCGGGGAGTACTACAT
mmu-miR-505-5p	GGGAGCCAGGAAGTATTGATAGT
mmu-miR-679-3p	AGCAAGGTCCTCCTCACATAGTA
mmu-miR-135b-5p	TATGGCTTTTCATTCTATGCCGC
mmu-miR-7239-5p	GCCATCCTGACAAAAGCTGATG
mmu-miR-691-F	ATTCCTGAAGAGAGGAGCTGA
IL25-F	CAGCAAAGAGCAAGAACCCC
IL25-R	CCGATTCAAGTCCCTGTCCAA

Vector construction and transfection

Sequences of IL-25 WT 3'UTR, bearing mutant site of mmu-miR-135b-5p or mmu-miR-691 were synthesized and cloned into pmirGLO (Promega, WI, USA) vector, resulting in Mus-IL-25 wt-pmirGLO, Mus-IL-25Mut-pmirGLO-135b, and Mus-IL-25Mut-pmirGLO-691 vectors. After the vectors were constructed, miRNA mimics, including mmu-miR-135b-5p, mmu-miR-691, and mmu-miRNA NC (negative control), synthesized by GenePharma, Shanghai, China were transfected or co-transfected with 100 nM Mus-IL-25 wt-pmirGLO, Mus-IL-25Mut-pmirGLO-135b, and Mus-IL-25Mut-pmirGLO-691 vectors using Lipofectamine 2000 (Invitrogen, CA, USA) into HEK-293 cells as per the manufacturer's instructions.

Luciferase report assay

For luciferase report assay, approximately 8000 cells were seeded on 96-well plates 8 h before the miRNA mimics and vectors transfection. miRNA mimics and vectors were transfected into HEK-293 as mentioned above. After 48 h of culture, luciferase activity was detected usingDual-Glo Luciferase Assay System (Promega, WI, USA) as per the manufacturer's instruction. The fluorescence values were calculated as firefly fluorescence value/Renilla fluorescence value.

Statistical analyses

Data are represented as mean \pm SD values, unless otherwise mentioned. The differences between the two groups were determined using 2-tailed Student's t tests. One-way ANOVAs analysis was used for making comparisons among more than three groups with SPSS version 12.0 (SPSS Inc.,

Chicago, IL, USA). P values < 0.05 were considered statistically significant.

Results

Establishment of a DSS-induced UC mice model

The UC mice model was constructed by adding DSS in the drinking water. After DSS administration, the body weight and DAI of the DSS-induced UC mice and the NC mice were recorded every day for 14 d. As shown in Figure 1, the weight of the NC mice showed no significant changes, while that of the DSS-induced UC mice showed a daily reduction after DSS induction, with the body weight becoming the lowest at 7 d after DSS treatment. After 7 d, the weight of the DSS-induced UC mice gradually recovered to a level similar to that in the NC mice (Figure 1(a)). The DAI of the NC group was 0 across the whole observation

period. Compared with the NC group, the DAI of the DSS group increased after DSS treatment and reached the highest value on the 7th day. After 7 d, the value dropped gradually; however, it was still higher than that in the NC group (Figure 1(b)).

After 7 d of DSS treatment, H&E results showed significant epithelial damage in the DSS group, significant loss of crypts, and separation from the muscularis mucosa (Figure 1(c)). In addition, the spleen weight had increased significantly and the colon was significantly shortened compared to that in the NC mice (Figure 1(d–f)). Obvious bloody stools were also observed in the DSS group.

A wide range of miRNA are differentially expressed in DSS-induced UC mice

Two mice in each group were subjected to miRNA sequencing. The results of miRNA sequencing

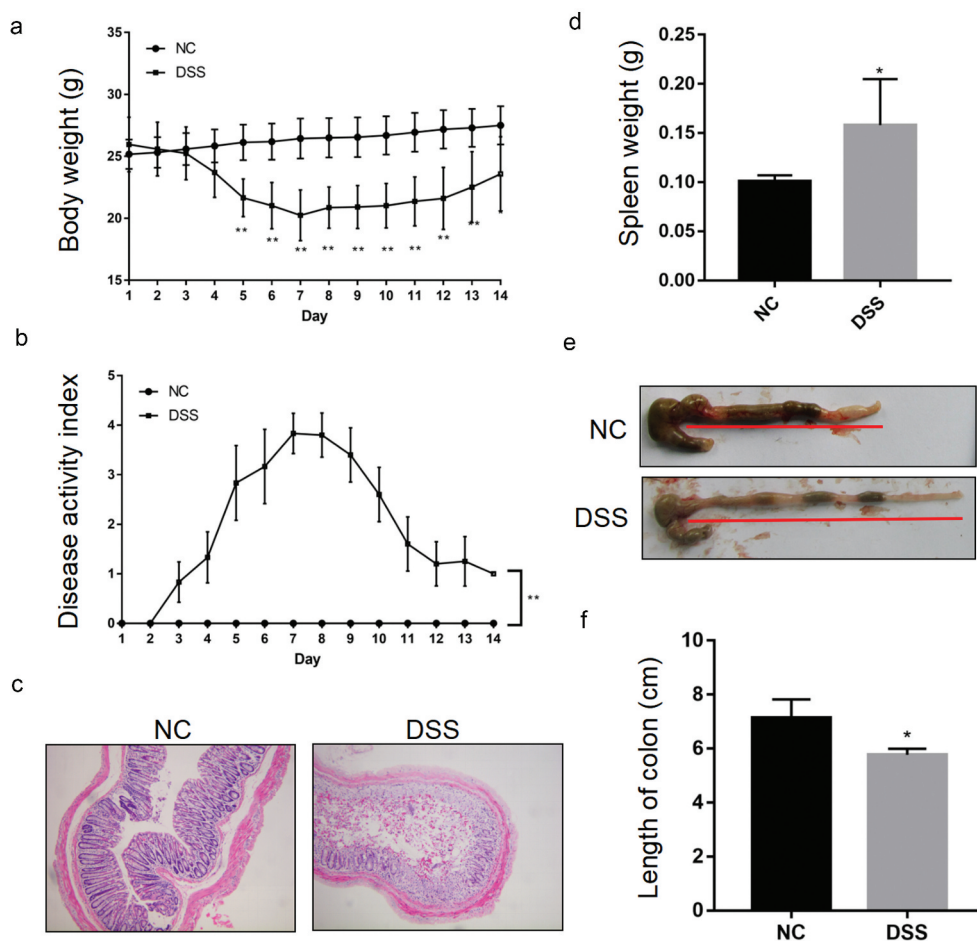


Figure 1. Successful construction of a DSS-induced UC mice model. Reduced body weight (a) and increased disease activity index (b) during a 14-day treatment period in the DSS feeding group (DSS). ** $P < 0.01$ vs. NC (ANOVA). (c) Representative image showing impaired epithelial integrity in the mucosa of DSS mice. Representative image showing increased spleen weight (d) and shortened colon length, indicated by red underline (e, f) in DSS mice compared with the normal feeding group (NC). * $P < 0.05$ vs. NC (t test).

showed that there were 95 differentially expressed miRNA, of which, 31 were up-regulated and 64 were down regulated. Heatmap revealed that the profile of miRNA expression in DSS-induced UC mice was different from that in the NC mice (Figure 2(a)).

To explore the function of these miRNAs that may be involved, miRNA targets were predicted, and the candidate miRNA targets were subjected to KEGG analysis. The KEGG result showed that these targets were mainly enriched in tumor-associated pathways, such as the pathway in cancer; the PI3K-AKT signaling pathway; immune pathways, such as the chemokine signaling pathway and the apoptosis signaling pathway (Figure 2(b)). Among the up-regulated miRNAs, the up-regulated levels of mmu-miR-135b-5p, mmu-miR-7239-5p, mmu-miR-3070-5p, mmu-miR-1983, and mmu-miR-882 were the highest.

IL-25 harbors the binding site of the miRNAs that were differentially expressed in UC mice

The target mRNA of the miRNA of the immune-related chemokine signaling pathway was further analyzed. First, the miRNA-mRNA interaction network of the chemokine signaling pathway gene was constructed. In this large interaction network, IL-25 links

the largest number of miRNAs. The most 25 up-regulated and down regulated miRNAs in the DSS rice (Table 2) and targeting 13 differentially expressed miRNAs (Figure 3(a)). Among them, 5 miRNAs were up-regulated and 8 were down regulated as per the miRNA sequencing results (Figure 3(b)). Moreover, RT-qPCR showed that mmu-miR-761, mmu-miR-7002-5p, mmu-miR-505-5p, and mmu-miR-679-3p were down regulated in the intestinal tissue of UC, while mmu-miR-135b-5p, mmu-miR-7239-5p, and mmu-miR-691 were up-regulated (Figure 3(c)). The IL-25 expression was also significantly decreased in the DSS mice.

The bioinformatics analyses suggested that there are binding sites between the up-regulated miRNAs and IL-25; therefore, we constructed a 3'UTR luciferase reporter vector containing the IL-25 wild and mutant sequences (Figure 4(a)) and co-transfected with miRNA mimics to HEK293 cells to validate the potential binding sites for IL-25 and miRNA. As shown in Figure 4, the luciferase activity of mmu-miR-135b-5p mimics+mus-IL-25 wt-pmirGL0 was significantly reduced compared to that of the NC mimics and mus-IL-25 wt-pmirGL0 co-transfection group. After IL-25 mutation, there was no significant change in the luciferase activity in the mus-IL-25mut-pmirGL0-135b+NC mimics group, while

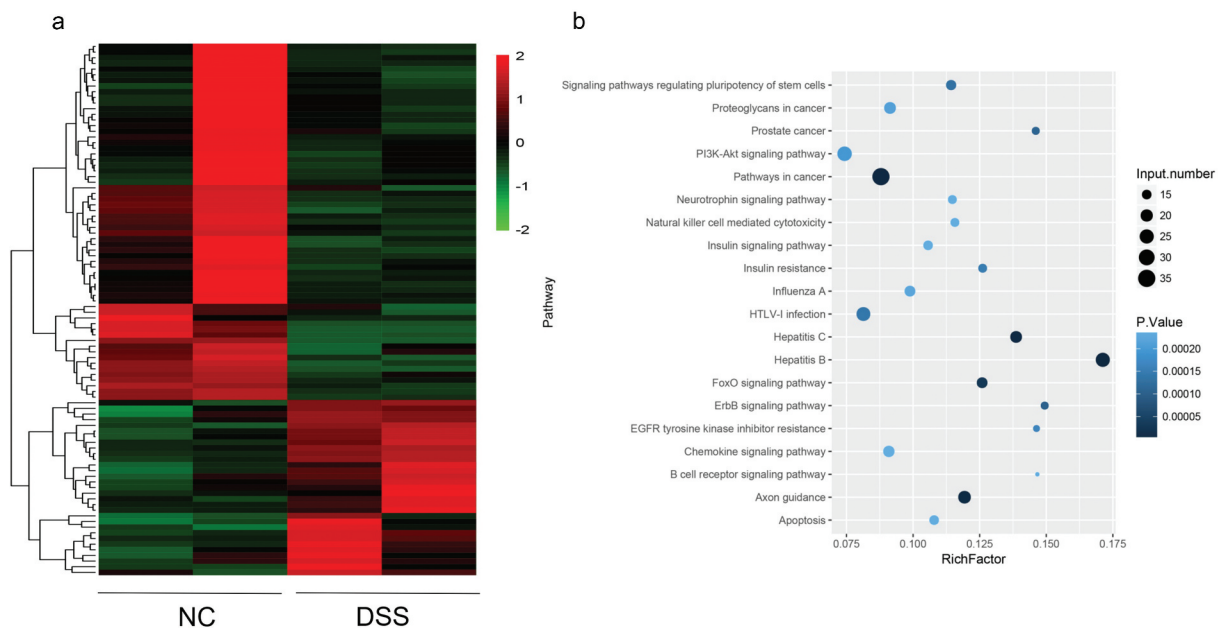


Figure 2. Differentially expressed miRNAs in UC mice screened by RNA sequencing. (a) Heat map showing an overview of differentially expressed miRNAs obtained from RNA sequencing data. The red and blue scales represent higher or lower expression levels, respectively. (b) KEGG pathway enrichment analysis showing the potential functions of these differentially expressed miRNAs and the pathways they may possibly be involved in.

Table 2. The most 25 up/down-regulated miRNAs in the DSS mice.

geneID	NC	DSS	Fold change (DSS/NC)	Up/Down regulation	P value
mmu-miR-135b-5p	2.54	11.15	4.39	Up	0.00
mmu-miR-7239-5p	3.85	13.58	3.53	Up	0.00
mmu-miR-3070-5p	2.95	9.34	3.17	Up	0.01
mmu-miR-1983	8.83	26.98	3.06	Up	0.03
mmu-miR-882	5.87	16.52	2.81	Up	0.02
mmu-miR-7668-3p	12.01	32.26	2.69	Up	0.04
mmu-miR-7661-3p	1.93	5.14	2.66	Up	0.01
mmu-miR-696	1.38	3.59	2.59	Up	0.00
mmu-miR-7084-5p	5.23	13.06	2.50	Up	0.03
mmu-miR-467a-3p	0.75	1.88	2.49	Up	0.01
mmu-let-7 k	4.40	10.90	2.48	Up	0.03
mmu-miR-467 f	0.35	0.85	2.43	Up	0.03
mmu-miR-6978-5p	2.70	6.56	2.43	Up	0.02
mmu-miR-6896-3p	2.42	5.79	2.40	Up	0.01
mmu-miR-466p-3p	0.63	1.50	2.38	Up	0.01
mmu-miR-669 g	0.49	1.17	2.37	Up	0.01
mmu-miR-877-5p	2.56	6.03	2.36	Up	0.02
mmu-miR-7033-3p	1.50	3.50	2.33	Up	0.01
mmu-miR-298-3p	2.63	5.99	2.28	Up	0.02
mmu-miR-34b-3p	1.67	3.75	2.24	Up	0.03
mmu-miR-691	1.40	3.03	2.16	Up	0.02
mmu-miR-3098-5p	1.86	4.01	2.16	Up	0.03
mmu-miR-6985-3p	2.88	6.09	2.11	Up	0.05
mmu-miR-6916-5p	0.90	1.87	2.07	Up	0.03
mmu-miR-761	4.19	1.70	0.41	Down	0.01
mmu-miR-7652-3p	10.49	4.19	0.40	Down	0.03
mmu-miR-302b-5p	8.35	3.27	0.39	Down	0.02
mmu-miR-615-3p	9.50	3.63	0.38	Down	0.02
mmu-miR-1264-3p	3.28	1.25	0.38	Down	0.01
mmu-miR-7228-3p	3.11	1.17	0.38	Down	0.00
mmu-miR-219a-2-3p	9.03	3.10	0.34	Down	0.01
mmu-miR-343	2.24	0.77	0.34	Down	0.00
mmu-miR-7064-5p	1.78	0.61	0.34	Down	0.00
mmu-miR-365-1-5p	4.40	1.49	0.34	Down	0.00
mmu-miR-7002-5p	8.89	2.94	0.33	Down	0.01
mmu-miR-802-5p	6.92	2.19	0.32	Down	0.01
mmu-miR-3080-3p	2.88	0.89	0.31	Down	0.00
mmu-miR-6947-3p	4.22	1.25	0.30	Down	0.00
mmu-miR-6924-3p	2.22	0.65	0.29	Down	0.00
mmu-miR-219b-5p	7.29	2.14	0.29	Down	0.00
mmu-miR-487b-5p	7.56	2.19	0.29	Down	0.00
mmu-miR-6946-5p	5.35	1.53	0.29	Down	0.00
mmu-miR-302 c-5p	1.71	0.48	0.28	Down	0.00
mmu-miR-383-3p	7.55	1.98	0.26	Down	0.00
mmu-miR-505-5p	3.46	0.85	0.25	Down	0.00
mmu-miR-10b-3p	29.01	6.91	0.24	Down	0.00
mmu-miR-10a-5p	17893.46	3872.45	0.22	Down	0.02
mmu-miR-10b-5p	5347.20	1106.07	0.21	Down	0.02
mmu-miR-7674-5p	7.46	1.38	0.18	Down	0.00
mmu-miR-10a-3p	277.22	41.18	0.15	Down	0.00

the luciferase activity of mus-IL-25mut-pmirGLO-135b+mmu-miR-135b-5p mimics cells was obviously restored. The same trend was also observed in the mmu-miR-691 group. The luciferase activity of mmu-miR-691 mimics+mus-IL-25 wt-pmirGLO was lower than that of NC mimics+mus-IL-25 wt-pmirGLO, while the luciferase activity of mmu-miR-691 mimics+mus-IL-25mut-pmirGLO-691 was significantly increased.

Discussion

In this study, we showed 94 differentially expressed miRNAs by comparing DSS-induced miRNA expression profiles in UC mice and normal mice. Of these, 31 were up-regulated and 64 were down regulated. The KEGG pathway enrichment analyses revealed that these differentially expressed miRNAs were mainly enriched in pathways such as those

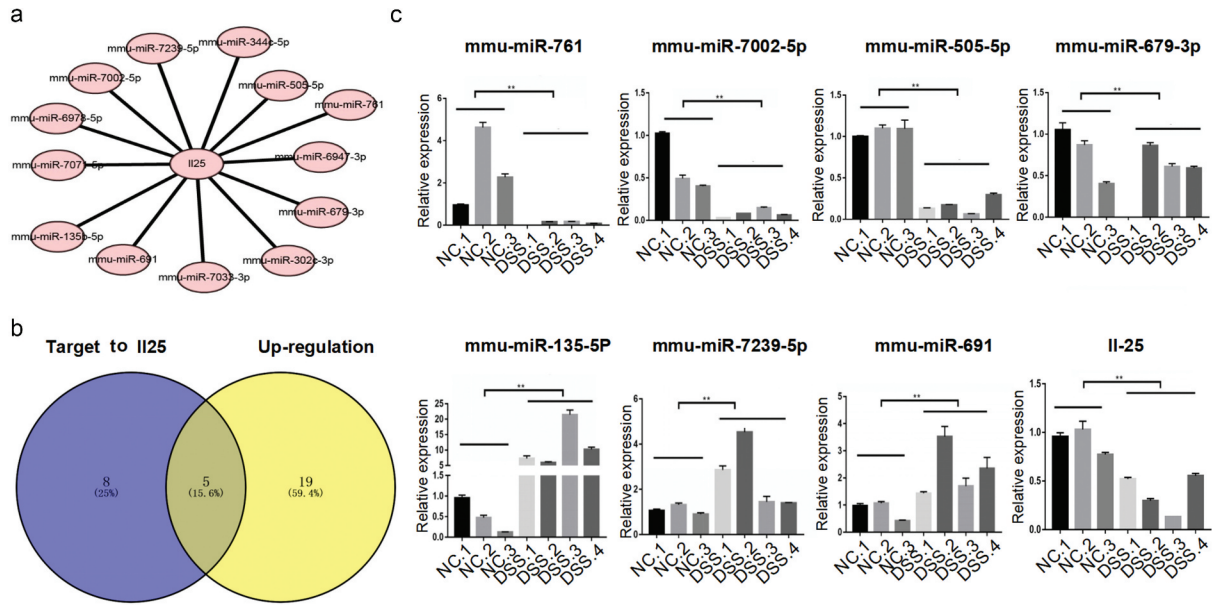


Figure 3. Bioinformatic and RT-qPCR analyses suggest that miRNAs are differentially expressed in UC mice and targets to IL-25. (a) Candidate interaction between miRNA and IL-25, a gene belonging to the chemokine pathway, were predicted using TargetsScan. (b) Common miRNAs among the up-regulated miRNAs were predicted using RNA-seq and bioinformatic targets of IL-25. (c) RT-qPCR assay differentially validated the expression of IL-25 and its candidate target miRNAs in DSS mice. **P < 0.01 vs. NC (ANOVA).

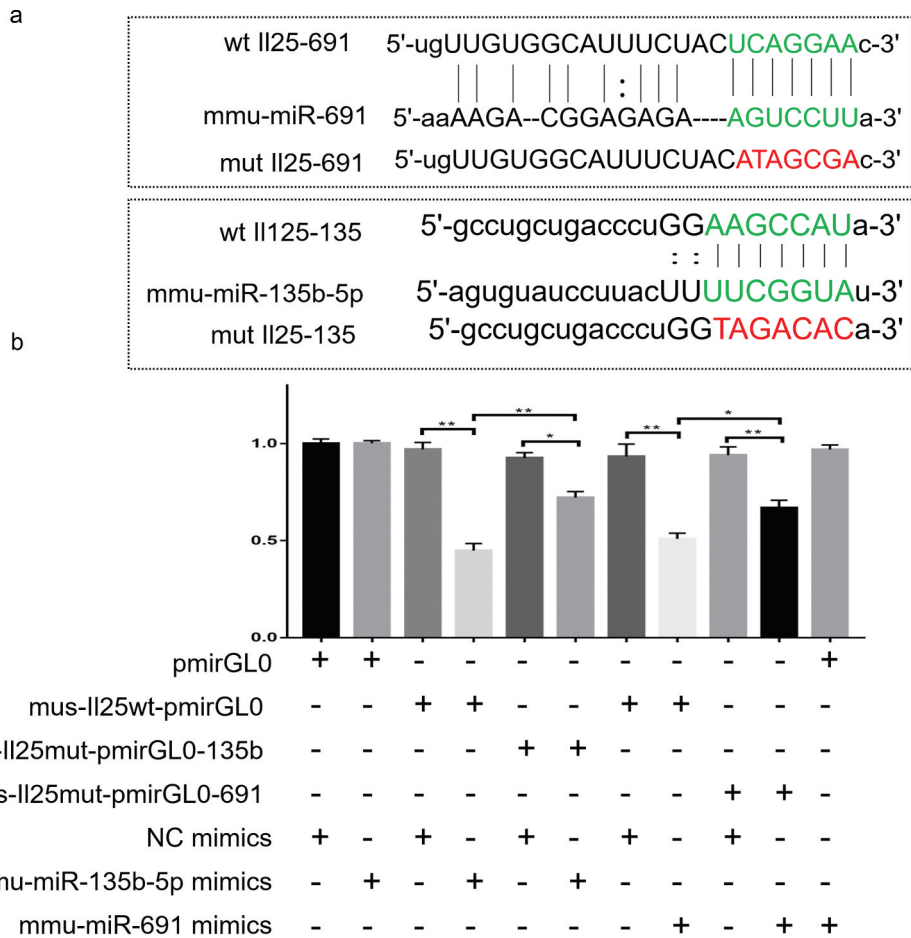


Figure 4. Luciferase assay showing the IL-25 and miR-691/miR-135b-5p relationship. (b) Candidate binding sites of IL-25 and miR-691/miR-135b-5p predicted by TargetsScan. (c) Luciferase report system verified the binding site of mmu-miR-691:IL-25 and mmu-miR-13b-5p:IL-25.

involved in tumor, proliferation, inflammation, and apoptosis. In particular, we analyzed the miRNA regulatory network in the chemokine signaling pathway and found that IL-25 regulates the largest number of bound miRNAs. Further, RT-qPCR results verified the downregulation of IL-25 and several target miRNAs of IL-25 in the intestinal tissue of UC mice; the expressions of mmu-miR-7002-5p, mmu-miR-505-5p, and mmu-miR-679-3p were down regulated, while those of mmu-miR-135b-5p, mmu-miR-7239-5p and mmu-miR-691 were up-regulated. Finally, we propose a regulatory relationship between mmu-miR-135b-5p: IL-25 and mmu-miR-691: IL-25.

Throughput sequencing revealed a series of differentially expressed miRNAs in UC. It is noteworthy that differentially expressed miRNAs are mainly enriched in tumors; PI3K-AKT signaling pathways; and inflammatory pathways, such as the chemokine signaling pathway and apoptotic pathways. Among them, the PI3K-AKT signaling pathway is involved in the regulation of apoptosis, inflammation, immunity, and barrier function in UC [15,16]. A previous web-based database study that compared the differences in the gene expressions of UC and CD found that chemokine receptor 7 (CCR7) and IL-8 of the chemokine pathway occupy important sites in the regulation of UC network. This finding suggests an important role of the chemokine signaling pathway in UC [17]. Apoptosis frequently occurring in the epithelial cells and lymphocytes is a common cell biological event that contributes to disrupted barrier function and UC development [18–22]. Our sequencing results also showed that DSS-induced UC differentially expressed miRNAs that may be involved in the regulation of apoptotic behavior.

UC is characterized by chronic relapsing intestinal inflammation. Therefore, we focus on the miRNAs involved in the chemokine signaling pathway. In the chemokine pathway, IL-25 is the most miRNA-targeted gene, suggesting its potential regulatory function in UC. IL-25 is a Th2-related factor that promotes the production of Th2 cytokines including IL-4, IL-13, and TGF- β 1 to alternatively activated macrophages [23]. It has been validated as downregulated in both sera and inflamed mucosa in patients with active IBD [24]. In the DSS-induced UC mouse model, IL-25 is

significantly downregulated and plays a role in inhibiting inflammatory factor IFN- γ and promoting the expression of anti-inflammatory factor IL-10 [25]. Another animal study shows that IL-25 can prevent intestinal inflammation [26]. Intraperitoneal injection of recombinant IL-25 has shown to relieve DAI, limit pathological changes, and prolong survival time in an acute UC mouse model [27]. These studies indicate that IL-25 plays the role of defending against the formation and progress of UC. However, the regulatory mechanism of IL-25 is not fully understood. In the current study, RT-qPCR assay confirmed the target miRNAs of IL-25, mmu-miR-761, mmu-miR-7002-5p, mmu-miR-505-5p, and mmu-miR-679-3p were down regulated, while those of mmu-miR-135b-5p, mmu-miR-7239-5p, and mmu-miR-691 were up-regulated in the intestinal tissues of UC mice. IL-25 was down regulated. This is consistent with the sequencing results. Mechanistically, miRNA acts as an mRNA level inhibitor by targeting the 3'UTR of mRNA. Therefore, we focused on the up-regulated miRNAs and verified the binding of miRNA and IL-25 using luciferase assay. Finally, we confirmed the relationship of mmu-miR-691: IL-25 and mmu-miR-135b-5p: IL-25. Although the function of mmu-miR-691 remains unclear, studies have suggested its up regulation upon PM2.5 intratracheal instillation and virus infection in mice, indicating its involvement in immune defense [28,29]. Another target of IL-25, mmu-miR-135b-5p, has been shown to be up-regulated in UC and IBD-associated tumor tissues [30–32] and is associated with colorectal cancer development and progression [33,34]. Currently, the exact role of mmu-miR-691 and mmu-miR-135b-5p in UC remains unknown. Our study confirms the interaction between mmu-miR-691/mmu-miR-135b-5p and IL25, indicating the role of mmu-miR-691 and mmu-miR-135b-5p in protecting against gut inflammation in the context of DSS-induced colitis.

Conclusions

In sum, we revealed the miRNA profile of UC in DSS-induced UC mice using high-throughput sequencing. Moreover, we predicted the

inflammation-related miRNA-IL-25 network and verified the regulatory relationship of mmu-miR-691:IL-25 and mmu-miR-13b-5p:IL-25. Current knowledge of miRNA-mRNA interaction in UC is limited. Our findings support that IL-25 is an important node of the UC inflammatory pathway, and this especially highlights the fact that the mmu-miR-691:IL-25 and mmu-miR-13b-5p:IL-25 networks have the potential to protect against UC, which may provide a clue for UC pathogen and targeted therapy analysis.

Highlights

- (1) A series UC associated miRNAs are found in DSS-Induce mice model.
- (2) IL-25 is a key target gene of UC associated miRNAs.
- (3) mmu-miR-135b-5p: IL-25 mmu-miR-691: IL-25 interactions are important pathways of UC development.

Author contributions

JY carried out most experiments, analyzed the data, and wrote the manuscript. DFL designed and supervised the study and wrote the manuscript. RYG supported cell culture assays. JYW and MHL performed mouse model. CW AND BHW performed bioinformatics. LLG performed RT-qPCR. LSW critically revised and finalized the manuscript.

Disclosure statement

The authors declare that they have no conflict of interest.

Funding

The study was supported by the national natural Science Foundation of China [No. 81800489], Three engineering training funds in Shenzhen [No. SYLY201718], Medical Scientific Research Foundation of Guangdong Province [No. A2020629] and Technical Research and Development Project of Shenzhen [Nos. JCYJ20170307100538697 and JCYJ20170307100911479].

References

- [1] Cohen RD, Yu AP, Wu EQ, et al. Systematic review: the costs of ulcerative colitis in Western countries. *Aliment Pharm Ther.* 2010;31:693–707.
- [2] Loddo I, Romano C. Inflammatory bowel disease: genetics, epigenetics, and pathogenesis. *Front Immunol.* 2015;6:551.
- [3] Gebert LF, MacRae IJ. Regulation of microRNA function in animals. *Nat Rev Mol Cell Biol.* 2018;20:21–37.
- [4] Garo LP, Murugaiyan G. Contribution of microRNAs to autoimmune diseases. *Cell Mol Life Sci.* 2016;73:2041–2051.
- [5] Xu X, Zhang H. miRNAs as new molecular insights into inflammatory bowel disease: crucial regulators in autoimmunity and inflammation. *World J Gastroenterol.* 2016;22:2206.
- [6] Takagi T, Naito Y, Mizushima K, et al. Increased expression of microRNA in the inflamed colonic mucosa of patients with active ulcerative colitis. *J Gastroenterol Hepatol.* 2010;25:S129–S133.
- [7] Koukos G, Polytarchou C, Kaplan JL, et al. A microRNA signature in pediatric ulcerative colitis: deregulation of the miR-4284/CXCL5 pathway in the intestinal epithelium. *Inflamm Bowel Dis.* 2015;21:996–1005.
- [8] Lee J, Park EJ, Yuki Y, et al. Profiles of microRNA networks in intestinal epithelial cells in a mouse model of colitis. *Sci Rep-Uk.* 2015;5:18174.
- [9] McKenna LB, Schug J, Vourekas A, et al. MicroRNAs control intestinal epithelial differentiation, architecture, and barrier function. *Gastroenterology.* 2010;139:1654–1664.
- [10] Soroosh A, Rankin CR, Polytarchou C, et al. microRNA-24 is elevated in ulcerative colitis patients and regulates intestinal epithelial barrier function. *Am J Pathol.* 2019;189:1763–1774.
- [11] Lin J, Welker NC, Zhao Z, et al. Novel specific microRNA biomarkers in idiopathic inflammatory bowel disease unrelated to disease activity. *Modern Pathol.* 2014;27:602.
- [12] Van der Goten J, Vanhove W, Lemaire K, et al. Integrated miRNA and mRNA expression profiling in inflamed colon of patients with ulcerative colitis. *Plos One.* 2014;9:e116117.
- [13] Gwiggner M, Martinez-Nunez R, Whiteoak S, et al. MicroRNA-31 and MicroRNA-155 are overexpressed in ulcerative colitis and regulate IL-13 signaling by targeting interleukin 13 receptor α -1. *Genes-Basel.* 2018;9:85.
- [14] Cai M, Chen S, Hu W. MicroRNA-141 is involved in ulcerative colitis pathogenesis via aiming at CXCL5. *J Interferon Cytokine Res.* 2017;37:415–420.
- [15] Chen Q, Duan X, Fan H, et al. Oxymatrine protects against DSS-induced colitis via inhibiting the PI3K/AKT signaling pathway. *Int Immunopharmacol.* 2017;53:149–157.
- [16] Chen T, Xue H, Lin R, et al. MiR-126 impairs the intestinal barrier function via inhibiting S1PR2 mediated activation of PI3K/AKT signaling pathway. *Biochem Biophys Res Commun.* 2017;494:427–432.
- [17] Cheng C, Hua J, Tan J, et al. Identification of differentially expressed genes, associated functional terms pathways, and candidate diagnostic biomarkers in

- inflammatory bowel diseases by bioinformatics analysis. *Exp Ther Med.* **2019**;18:278–288.
- [18] Vetuschi A, Latella G, Sferra R, et al. Increased proliferation and apoptosis of colonic epithelial cells in dextran sulfate sodium-induced colitis in rats. *Dig Dis Sci.* **2002**;47:1447–1457.
- [19] Wu F, Huang Y, Dong F, et al. Ulcerative colitis-associated long noncoding RNA, BC012900, regulates intestinal epithelial cell apoptosis. *Inflamm Bowel Dis.* **2016**;22:782–795.
- [20] Qiu W, Wu B, Wang X, et al. PUMA-mediated intestinal epithelial apoptosis contributes to ulcerative colitis in humans and mice. *J Clin Invest.* **2011**;121:1722–1732.
- [21] Qi TY, Saruta M, Papadakis KA. Visilizumab induces apoptosis of mucosal T lymphocytes in ulcerative colitis through activation of caspase 3 and 8 dependent pathways. *Clin Immunol.* **2008**;127:322–329.
- [22] Schulzke JD, Bojarski C, Zeissig S, et al. Disrupted barrier function through epithelial cell apoptosis. *Ann Ny Acad Sci.* **2006**;1072:288–299.
- [23] Rizzo A, Monteleone I, Fina D, et al. Inhibition of colitis by IL-25 associates with induction of alternatively activated macrophages. *Inflamm Bowel Dis.* **2012**;18:449–459.
- [24] Su J, Chen T, Ji X, et al. IL-25 downregulates Th1/Th17 immune response in an IL-10–dependent manner in inflammatory bowel disease. *Inflamm Bowel Dis.* **2013**;19:720–728.
- [25] Mchenga SS, Wang D, Janneh FM, et al. Differential dose effects of recombinant IL-25 on the development of dextran sulfate sodium-induced colitis. *Inflamm Res.* **2010**;59:879–887.
- [26] Camelo A, Barlow JL, Drynan LF, et al. Blocking IL-25 signalling protects against gut inflammation in a type-2 model of colitis by suppressing nuocyte and NKT derived IL-13. *J Gastroenterol.* **2012**;47:1198–1211.
- [27] Mchenga SS, Wang D, Li C, et al. Inhibitory effect of recombinant IL-25 on the development of dextran sulfate sodium-induced experimental colitis in mice. *Cell Mol Immunol.* **2008**;5:425.
- [28] Hou T, Liao J, Zhang C, et al. Elevated expression of miR-146, miR-139 and miR-340 involved in regulating Th1/Th2 balance with acute exposure of fine particulate matter in mice. *Int Immunopharmacol.* **2018**;54:68–77.
- [29] Zhao P, Zhao L, Zhang K, et al. Infection with street strain rabies virus induces modulation of the microRNA profile of the mouse brain. *Virol J.* **2012**;9:159.
- [30] Fasseu M, Treton X, Guichard C, et al. Identification of restricted subsets of mature microRNA abnormally expressed in inactive colonic mucosa of patients with inflammatory bowel disease. *Plos One.* **2010**;5:e13160.
- [31] Min M, Peng L, Yang Y, et al. MicroRNA-155 is involved in the pathogenesis of ulcerative colitis by targeting FOXO3a. *Inflamm Bowel Dis.* **2014**;20:652–659.
- [32] Olaru AV, Selaru FM, Mori Y, et al. Dynamic changes in the expression of MicroRNA-31 during inflammatory bowel disease-associated neoplastic transformation. *Inflamm Bowel Dis.* **2010**;17:221–231.
- [33] Xu XM, Qian JC, Deng ZL, et al. Expression of miR-21, miR-31, miR-96 and miR-135b is correlated with the clinical parameters of colorectal cancer. *Oncol Lett.* **2012**;4:339–345.
- [34] Li J, Liang H, Bai M, et al. miR-135b promotes cancer progression by targeting transforming growth factor beta receptor II (TGFB2) in colorectal cancer. *Plos One.* **2015**;10:e130194.